https://doi.org/10.20965/ijat.2020.p1005

Paper:

Model-Based Deterioration Estimation with Cyber Physical System

Tomoaki Hiruta*,† and Yasushi Umeda**

*Research & Development Group, Hitachi Ltd.
7-1-1 Omika-cho, Hitachi, Ibaraki 319-1292, Japan
†Corresponding author, E-mail: tomoaki.hiruta.dp@hitachi.com
**Research into Artifacts, Center for Engineering, School of Engineering, The University of Tokyo, Tokyo, Japan

[Received April 26, 2020; accepted June 23, 2020]

A key aspect of life cycle management for pursuing sustainability is machine condition prognosis, which requires a condition monitoring system that estimates machine system deterioration to assist engineers in determining which maintenance actions to take. Conventional data-driven methods such as machine learning, have two issues. One is data dependency. The accuracy of a data-driven method depends on the data volume because a data-driven method builds a classification model on the basis of historical data as training data. However, it is difficult to acquire enough data on all deterioration modes, which requires a long time, because deterioration modes are diverse, and some of them rarely happen. The other issue is interpretability. When a condition monitoring system using a data-driven method sends the degree of deterioration (DoD) of the machine system to maintenance engineers, they have difficulty in understanding the results because the method is a black box. The objective of this paper is to address these two issues. We propose a model-based method that simulates machine system deterioration with a cyber physical system (CPS). Model-based methods address these issues in the following manner. First, the methods can simulate the progress of deterioration from an initial condition to failure to estimate the DoD. Second, the methods employ mathematical models that represent machine systems. Engineers create such mathematical models (which we call "physical models") by referring to various kinds of knowledge like design information and the result of failure mode and effects analysis. A physical model allows us to reason about a machine system to address interpretability. For dealing with machinery that has multiple operation modes, we introduce a state space to clarify the relationship among input, observable state variables, and DoD in a physical model. The CPS estimates DoD by comparing observed data with simulated data in the state space. In our case study, we evaluated our proposed method with a hydraulic pump of a mining machine. First we created a physical model with Modelica, which is a multi-domain modeling language. Then, the method constructed the state space by simulating deterioration with the physical model given all combinations of inputs and DoD. After that, we showed that the estimated DoD tended to increase until the hydraulic pump was replaced, using the observed data from an actual mining machine. As a result, the experimental results revealed that the proposed method succeeded in identifying the DoD with observed data of the hydraulic pump of a mining machine.

Keywords: maintenance, deterioration, cyber physical system

1. Introduction

Life cycle engineering [1, 2] is a key concept for promoting environmentally sustainable practices among manufacturers because maintenance in the middle of a product's life cycle is essential for efficiently extending its lifetime. Much recent research has focused on condition-based maintenance, which contributes to increasing the availability of machines and reducing maintenance costs through the use of a condition monitoring system [3–5].

In condition-based maintenance, a condition monitoring system assists maintenance engineers in determining the right maintenance actions to be taken at the right time [6, 7]. The core task of recent condition monitoring systems is to estimate the deterioration of machine systems with data collected from machine systems. Many data-driven methods have been proposed for estimating deterioration. An example is machine learning based anomaly detection, which identifies unusual machine conditions that do not conform to expected machine system behavior [8]. In this method, first, a machine learning technique creates patterns for a machine system under normal conditions. Then, in operation mode, it detects differences from these patterns as machine system condition anomalies [9, 10]. For condition-based maintenance of medical equipment, data scientists designed a data analytics process for predicting equipment failure with equipment operation logs and machine learning algorithms [11].

However, such data-driven methods have two issues.

One is data dependency. The accuracy of a data-driven method depends on the data volume. However, it is difficult to acquire enough data on all deterioration modes, which requires a long time, because deterioration modes are diverse, and some of them rarely happen. For example, if deterioration mode "A" happens at 10^{-4} percent per hour, it would take 1.14 years to acquire one sample for this mode. For dealing with various kinds of deterioration modes, data acquisition requires more time than the product lifetime.

The other issue is interpretability. When a condition monitoring system using a data-driven method sends the degree of deterioration (DoD) of the machine system to maintenance engineers, the engineers have difficulty in understanding the reason why the system detect that DoD, because the method is a black box.

Model-based methods address these issues in the following manner. First, the model-based methods simulate machine behavior as deterioration progresses from an initial condition to failure. This can avoid the long-time data collection. Second, the model-based methods employ mathematical models that represent a mechanical system, so they allow us to reason about the system. Hence, we take an model-based approach.

Conventional model-based methods have been proposed for simple machine elements with experimental data rather than actual operational data. One example is a bearing-faults model that provided simulated data for creating a fault classification, which is a supervised machine learning method [12]. Another example is an electric circuit deterioration model that was utilized with a causal network and experimental data [13]. Furthermore, one example of model-based methods utilized simulated data of aircraft engine modules for the damage propagation [14].

However, few researchers have dealt with machine systems rather than machine elements with observed data collected from actual machines. For dealing with observed data of machine systems in a model-based methods, we need to address two issues. First, there is a gap between observed data and simulated data, which leads to inaccurate DoD estimation. Second, a machine system has multiple operation modes. It is difficult to recognize operation modes with a time series of observed data.

In this paper, we propose a model-based method for estimating deterioration with a cyber physical system (CPS) [15]. We describe mathematical models (we call "physical models") with mathematical equations with multi-domain modeling language to simulate normal and deteriorated machine behavior. To fill the gap between observed and simulated data, we utilize a methodology of combining observed and simulated data called "data assimilation" [16]. Data assimilation is used to estimate the state of a complex system such as the atmosphere from observed data and physical models [17]. Specifically, we estimate the attributes of a physical model for matching simulated data to observed data as described in Section 2.2.4.

Moreover, the method introduces a state space with simulated and observed data to deal with multiple operation modes of machine systems such as power plants, medical equipment, mining machinery, automobiles, and motors.

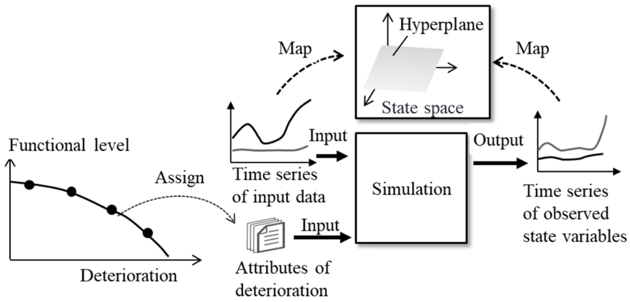

Fig. 1. Simulation with discretized attributes of deterioration to create state space.

The paper is structured as follows. Section 2 proposes the deterioration estimation method with CPS. Section 3 shows a case study of a hydraulic pump, and the proposed method is evaluated with observed data from the physical world. Section 4 discusses the contributions to maintenance operation and the limitations of the proposed method. Section 5 concludes this paper.

2. Model-Based Deterioration Estimation Method

Our approach integrates a physical model of machine system in the cyber world and observed data in the physical world to address the issues with data dependency and the interpretability of deterioration estimations. Specifically, we take the approach as shown in **Fig. 1**. First, we discretize the progress of deterioration for a machine system. Then we construct state space by executing a model-based simulation with the discretized values of deterioration. The state space is used for estimating deterioration with observed data.

Our method consists of two phases: preparation and execution. After constructing the CPS for estimating deterioration in the preparation phase, engineers create a physical model and construct the state space. Then, in the execution phase, the CPS identifies the DoD by positioning the observed data from the machine in the state space.

2.1. Cyber Physical System for Deterioration Estimation

Figure 2 shows the CPS for estimating deterioration for condition-based maintenance. The cyber world contains the physical model and the state space. When the cyber world receives observed data from the physical world, it estimates the DoD of the machine system in the state space.

In the physical world, when maintenance engineers receive information about the DoD of a machine system, they send work orders to maintenance workers, who conduct maintenance on the machine system.

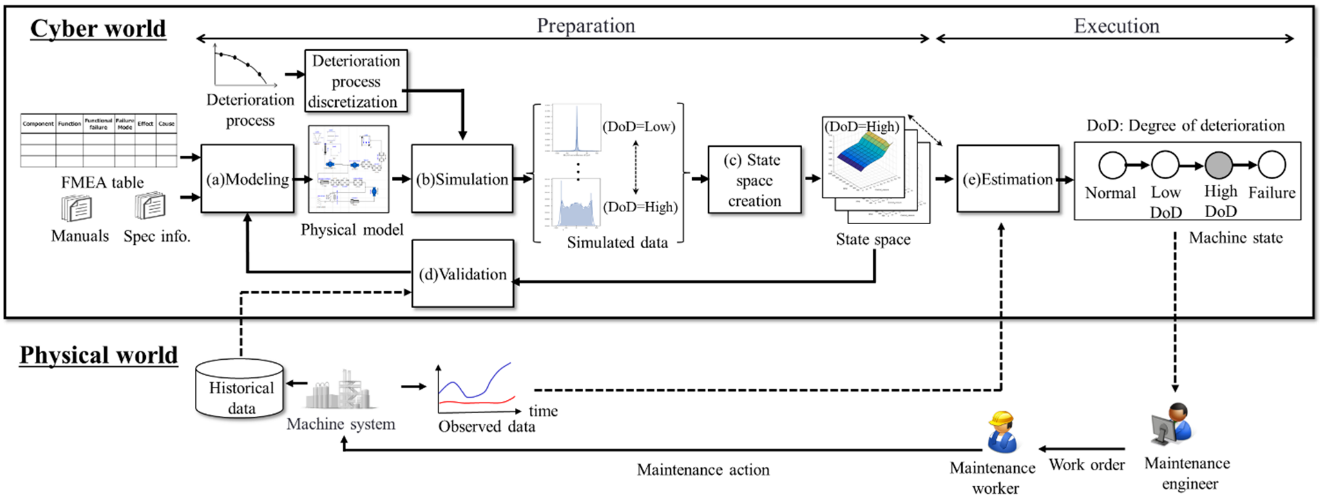

Fig. 2. Cyber physical system for estimating machine system deterioration.

2.2. Preparation Phase

The preparation phase consists of four sub-phases: (a) modeling, (b) simulation, (c) state space creation, and (d) validation as shown in **Fig. 2**.

2.2.1. Modeling

In the modeling phase, engineers create a physical model by referring to various kinds of knowledge like design information and the results of failure mode and effects analysis (FMEA) [18].

The physical model represents the machine system behavior as shown in Eqs. (1) and (2).

$$\dot{\boldsymbol{x}}(t) = f(\boldsymbol{x}(t), \boldsymbol{u}(t), \boldsymbol{p}, \boldsymbol{d}), \quad \ldots\ldots\ldots \quad (1)$$

$$\dot{\boldsymbol{d}} = g(\tau, \boldsymbol{d}, \boldsymbol{u}(\tau), \boldsymbol{x}(\tau), \boldsymbol{p}). \quad \ldots\ldots\ldots \quad (2)$$

where $\boldsymbol{u}(t) = [u_1(t), \ldots, u_M(t)]^T$ represents the input vector of the machine system in the physical model at time t; M represents the number of input parameters; $\boldsymbol{x}(t) = [x_1(t), \ldots, x_N(t)]^T$ represents the state variable vector at time t; N represents the number of variable parameters; $\boldsymbol{p}$ represents the attributes of the physical model; $\boldsymbol{d} = [d_1, \ldots, d_L]^T$ represents the attributes of deterioration, which is defined as DoD; L represents the number of attributes of deterioration; $f(\cdot)$ represents the behavior of the machine system in operation; $g(\cdot)$ is a function representing deterioration progress of the physical model. In Eq. (2), $\boldsymbol{d}$ depends on time τ, $\boldsymbol{u}(\tau)$, $\boldsymbol{x}(\tau)$, and $\boldsymbol{p}$.

We assumed that time t in Eq. (1) represents the time for the operation of the machine system. On the other hand, time τ in Eq. (2) represents a longer time for the deterioration progress. Hence, Eq. (1) deals with $\boldsymbol{d}$ as constant, and $\boldsymbol{d}$ changes according to time and machine operation as shown in Eq. (2). Moreover, we introduce $\boldsymbol{y}(t) = [y_1(t), \ldots, y_O(t)]^T$ representing the observable state variable vector, $\boldsymbol{y}(t) = \{y \| y \in \boldsymbol{x}(t), y \text{ is observable}\}$. O represents the number of observable state variable parameters. Note that we assume $\boldsymbol{u}(t)$ is also observable in this paper.

In the modeling sub-phase, engineers first describe the physical model. Then, they select the target failure modes related to deterioration that have critical impacts and high probability by using an FMEA table and describe them as $\boldsymbol{d}$. For example, when the target failure mode is the wear of a brake pad, its $\boldsymbol{d}$ can be represented as a friction coefficient.

2.2.2. Simulation

In the simulation, for acquiring all possible values of observable state variable vector $\boldsymbol{y}(t)$, the engineers simulate all possible patterns of the values of input vector $\boldsymbol{u}(t)$ and $\boldsymbol{d}$ in the cyber world.

Considering the calculation cost, the engineers discretize values of input vector $\boldsymbol{u}(t)$ and $\boldsymbol{d}$. Specifically, $u_m(t, k_m)$ represents the k_m-th bin of input parameter u_m ($k_m = 1, \ldots, K_m$), and $d_l(k_l)$ represents the k_l-th bin of DoD d_l ($k_l = 1, \ldots, K_l$). The physical model simulates the observable state variable vector $\boldsymbol{y}(t, k, k_l)$ given all combinations of the k-th input vector $\boldsymbol{u}(t, k)$ and the k_l-th DoD $d_l(k_l)$.

2.2.3. State Space Creation

The observable state variable vectors $\boldsymbol{y}(t)$ and state variables $\boldsymbol{x}(t)$ are affected by $\boldsymbol{u}(t)$ and $\boldsymbol{d}$. Assuming that the operation mode of a machine system (e.g., a boiler) is constant, we can estimate $\boldsymbol{d}$ only with $\boldsymbol{y}(t)$. However, in the case of machinery that has multiple operation modes (e.g., a mining machine), it is necessary to focus on the relationship between $\boldsymbol{u}(t)$ and $\boldsymbol{y}(t)$ for estimating $\boldsymbol{d}$. Therefore, we introduce the state space to clarify the relationship among input, observable state variables, and DoD.

In state space creation, the engineers execute projection from $\boldsymbol{u}(t)$ and $\boldsymbol{y}(t)$ into the state space. As a result, machine system behavior is expressed as a hyperplane in the state space. **Fig. 3** shows an overview of projection from

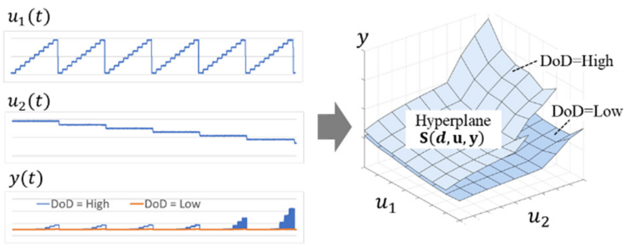

(A) Time-series data (B) State space

Fig. 3. Overview of projection from simulated observable state variables $\boldsymbol{y}(t)$ and input $\boldsymbol{u}(t)$ (A) into hyperplanes in state space (B).

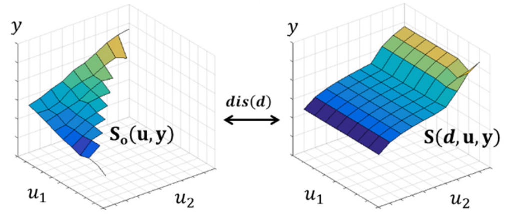

Observed data in state space Simulated data in state space

Fig. 4. Finding suitable $\boldsymbol{d_{min}}$ after calculating difference $\boldsymbol{dis}(\boldsymbol{d})$ between observed and simulated data in state space.

simulated observable state variables $\boldsymbol{y}(t)$ and input $\boldsymbol{u}(t)$ (**Fig. 3(A)**) into hyperplanes in the state space (**Fig. 3(B)**). Here, $\boldsymbol{S}(\boldsymbol{d},\boldsymbol{u},\boldsymbol{y})$ represents a hyperplane simulated with a physical model given $\boldsymbol{d}$. In the state space, the DoD of a machine system is expressed as a change in the hyperplane as shown in **Fig. 3(B)**.

2.2.4. Validation

In the validation phase, engineers calibrate attributes $\boldsymbol{p}$ with historical data under normal machine behavior ($\boldsymbol{d} = \boldsymbol{d_{normal}}$). The engineers assign the attributes $\boldsymbol{p}$ to minimize the difference $\boldsymbol{dis}(\boldsymbol{d_{normal}})$ between the hyperplane $\boldsymbol{S_o}(\boldsymbol{u},\boldsymbol{y})$ of the historical data and that $\boldsymbol{S}(\boldsymbol{d_{normal}},\boldsymbol{u},\boldsymbol{y},)$ of the simulated data with Eq. (3).

$$\boldsymbol{dis}(\boldsymbol{d}) = \sqrt{\sum_{\boldsymbol{u},\boldsymbol{y}} \boldsymbol{n_{u,y}} \left(\boldsymbol{S_o}(\boldsymbol{u},\boldsymbol{y}) - \boldsymbol{S}(\boldsymbol{d},\boldsymbol{u},\boldsymbol{y})\right)^2} \quad . \quad (3)$$

where $\boldsymbol{n_{u,y}}$ represents the number of observed data assigned to the hyperplane $\boldsymbol{S_o}(\boldsymbol{u},\boldsymbol{y})$. Observed data assigned to grids on the hyperplane $\boldsymbol{S_o}(\boldsymbol{u},\boldsymbol{y})$ are imbalanced. To deal with imbalanced data, we utilize weighed sum with $\boldsymbol{n_{u,y}}$ in Eq. (3).

2.3. Execution

In the execution phase, the CPS identifies the DoD with observed data and the state space. Observed data is collected from the machine system through information and communications technologies (ICT) in the CPS.

To find the DoD $\boldsymbol{d_{min}}$ of the smallest distance between the hyperplane $\boldsymbol{S_o}(\boldsymbol{u},\boldsymbol{y})$ of the observed data and that $\boldsymbol{S}(\boldsymbol{d},\boldsymbol{u},\boldsymbol{y})$ of the simulated data, the optimization problem can be formalized as follows:

$$\begin{aligned} &\boldsymbol{d_{min}} = \arg\min\ \boldsymbol{dis}(\boldsymbol{d}) \\ &\text{s.t.} \quad d_l \in \{d_l(1),\ldots,d_l(K_l)\}, \quad \forall \boldsymbol{u} \end{aligned} \quad . \ . \ . \ . \ (4)$$

In this paper, the engineers select $\boldsymbol{d_{min}}$ with an exhaustive search of discretized input $\boldsymbol{u}$, $\boldsymbol{y}$ and $\boldsymbol{d}$. **Fig. 4**. shows an overview of the calculation between the observed and simulated data in the state space. The difference $\boldsymbol{dis}(\boldsymbol{d})$ in Eq. (3) is calculated from input of observed data in the state space ($\boldsymbol{n_{u,y}} > 0$).

3. Case Study

We evaluated our proposed method with a hydraulic pump of a mining machine. The pump can transform rotational energy from an engine into hydraulic energy to control a connected actuator. If this pump breaks down, the machine will stop, which would lead to low availability. Therefore, condition-based maintenance is needed.

3.1. Hydraulic Pump and its Modeling

In this case study, the type of hydraulic pump was a variable displacement pump with a swash plate that operates a displacement axial piston to control the flow rate [19].

Table 1 shows the input, observable state variables, attributes and DoD of the physical model based on Eqs. (1) and (2). **Fig. 5** shows the mechanism of the hydraulic pump. The input to the hydraulic pump is the time-series data of rotational speed $u_1(t)$ from the engine and the desired pump pressure $u_2(t)$ controlled by the mining machine operator. The hydraulic pump state variables were the flow rate, pump pressure, drain flow rate, and pushing area controlled by the swash plate. We manually set attributes based on design information of the hydraulic pump. Moreover, on the basis of discussion with domain engineers and the mechanism shown in **Fig. 5**, we selected drain pressure as the observable state variable of the hydraulic pump $\boldsymbol{y}(t)$. Drain pressure is the pressure from internal oil leakage from the pump. Note that the pump pressure is not an indicator for identifying DoD because the controller controls the swash plate angle to achieve the desired pump pressure. As a result, the pump pressure is not directly influenced by DoD. Drain pressure is observable in the physical world and is affected by the pump volumetric efficiency η_v described below.

In this case study, we focused on the wear of a piston as the target failure mode on the basis of discussion with domain engineers. We decided to describe the degree of piston surface wear as the pump volumetric efficiency η_v. Namely, d_1 was defined as $(1-\eta_v)$ in the physical model. When η_v was close to 0 (d_1 was close to 1), the piston condition reaches failure.

3.2. Construction of Physical Model

We created the physical model with Modelica [20, 21], which is a multi-domain modeling language as shown in

Table 1. Parameters of physical model of hydraulic pump.

Category	Variables	Description
Input	$u_1(t)$	Rotational speed from engine.
	$u_2(t)$	Desired pump pressure from operator.
State variables	$x_1(t)$	Flow rate.
	$x_2(t)$	Pump pressure.
	$x_3(t)$	Drain flow rate.
	$x_4(t)$	Pushing area controlled by swash plate.
	$x_5(t)$	Drain pressure.
DoD	d_1	$d_1 = 1 - \eta_v$ η_v represents pump volumetric efficiency that ranges from 0.0 to 1.0.
Observable state variables	$y_1(t)$	Drain pressure.
Attributes of the hydraulic pump	$\boldsymbol{p}$	- Gain of controller. - Mathematical relationship between pump pressure and flow rate of piston.

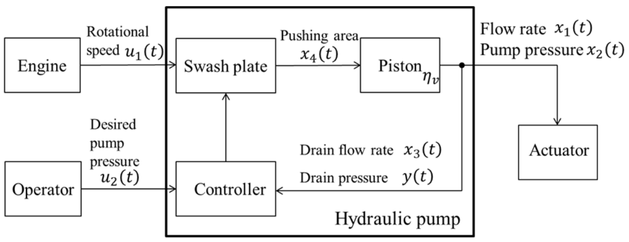

Fig. 5. Mechanism of hydraulic pump.

Fig. 6. Modelica allows us to describe multi-domain components as a physical model. In this case study, the physical model of the hydraulic pump consisted of a controller and mechanical components, i.e., a swash plate and piston.

To reduce the noise from historical and observed data, in preparing data, we calculated the average value of the historical and the observed data with a time window.

Finally, we validated the physical model by minimizing $\boldsymbol{dis}(\boldsymbol{d_{normal}})$ between the hyperplane $\boldsymbol{S}(\boldsymbol{d_{normal}}, \boldsymbol{u}, \boldsymbol{y})$ of the simulated data and that $\boldsymbol{S_o}(\boldsymbol{u}, \boldsymbol{y})$ of the historical data for the normal machine condition (DoD $\boldsymbol{d} = \boldsymbol{d_{normal}}$) with Eq. (3). In this study, we assumed that $\boldsymbol{d_{normal}}$ was 0.05 ($\boldsymbol{d_{normal}} = 1 - 0.95$), because the pump volumetric efficiency η_v of a new hydraulic pump is 0.95 [19]. **Fig. 7** shows a relationship between the difference $\boldsymbol{dis}(\boldsymbol{d})$ and DoD $\boldsymbol{d}$. The difference $\boldsymbol{dis}(\boldsymbol{d})$ is minimum when DoD $\boldsymbol{d}$

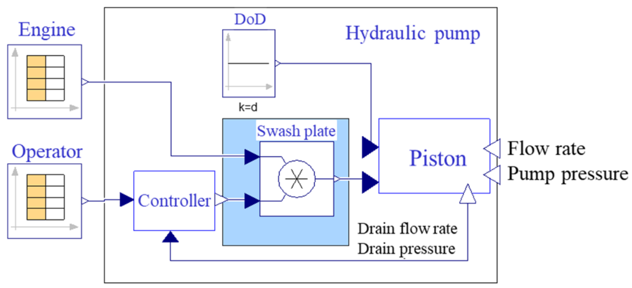

Fig. 6. Pheysical model of hydraulic pump with Modelica [20, 21].

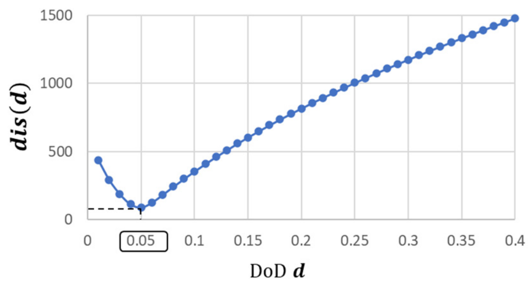

Fig. 7. Relationship between the difference $\boldsymbol{dis}(\boldsymbol{d})$ and DoD $\boldsymbol{d}$ for physical model validation.

is 0.05.

After the validation, we compared the historical and simulated pump pressure as shown in **Fig. 8**. **Fig. 8(a)** shows time-series data of the observed and simulated data pump pressure. **Fig. 8(b)** indicates that the correlation coefficient between them was 0.981. This means that the physical model well represented the pump in the physical world.

3.3. Simulation of Deterioration

First, we discretized the values of the input and observable state variables to create hyperplanes in the state space. In particular, each input variable was discretized into 10 bins considering the calculation cost and data distribution. Hence, the input data had 100 patterns of $u_1(t, k_1)$ and $u_2(t, k_2)$ $(k_1, k_2 = 1, \ldots, 10)$. For example, when the observed engine rotational speed $u_1(t)$ ranges from 0 to 3000 rpm, each bin has 300 rpm buckets. And engine rotational speed $u_1(t)$ from 0 to 300 rpm was represented as $u_1(t, 1)$.

We prepared 20 patterns of DoD from 0.05 (normal) to 0.40 (failure) according to the specifications of the hydraulic pump.

After discretizing the input and DoD, the physical model simulated the observable state variables $\boldsymbol{y}(t, k_{u1}, k_{u2}, k_l)$ given all combinations of the k_{u1}-th and k_{u2}-th inputs and the k_l-th DoD d_1.

3.4. State Space Creation

The simulated data of each DoD d_1 was mapped onto the hyperplane $\boldsymbol{S}(d_1, \boldsymbol{u}, \boldsymbol{y})$ in the state space. In this study,

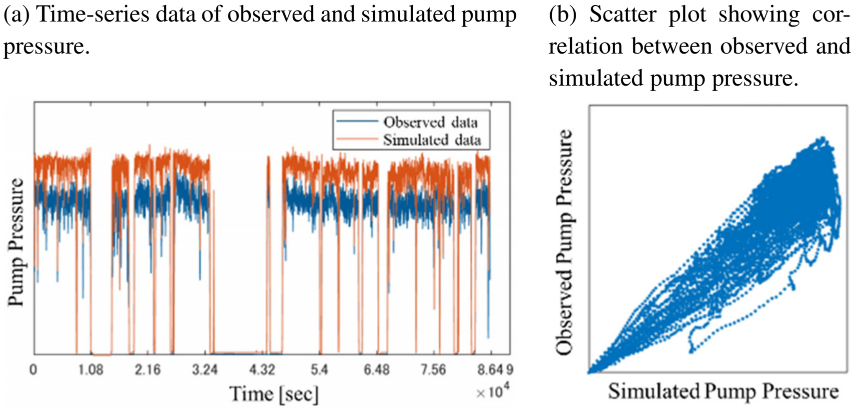

Fig. 8. Time-series data and scatter plot of main pump pressure for physical model validation.

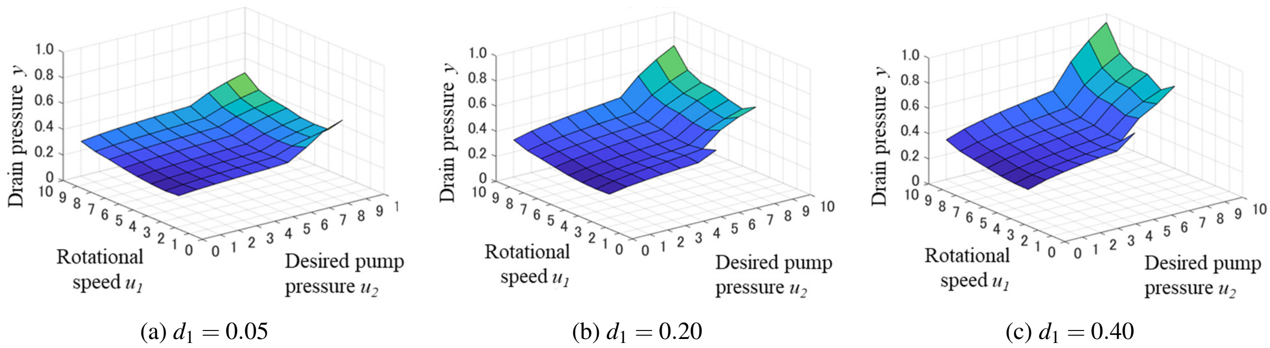

Fig. 9. Examples of hyperplanes created by simulated data in state space for each DoD ($d_1 = \{0.05, 0.20, 0.40\}$).

the state space had three axes: input rotational speed u_1, desired pump pressure u_2, and drain pressure $\boldsymbol{y}$.

Figure 9 shows examples of hyperplanes $\boldsymbol{S}(d_1, \boldsymbol{u}, \boldsymbol{y})$ in the state space of each DoD $d_1 = \{0.05, 0.20, 0.40\}$. The figure reveals that the hyperplanes in the state space depended on the input, observable state variables, and the DoD of the hydraulic pump of the mining machine.

3.5. Estimation of Degree of Deterioration

We acquired 116 days of observed data out of 589 days from an actual mining machine. After the pump broke down on the 513th day, a maintenance worker replaced it with a new one.

In accordance with Eq. (3), we calculated the distance $\boldsymbol{dis}(d_1)$ between the observed data $\boldsymbol{S_o}(\boldsymbol{u}, \boldsymbol{y})$ from the dataset and the simulated data $\boldsymbol{S}(d_1, \boldsymbol{u}, \boldsymbol{y})$ of each DoD d_1. Then, we selected the estimated DoD $\boldsymbol{d_{min}}$ of each piece of observed data with Eq. (4).

Figure 10 shows the estimated DoD $\boldsymbol{d_{min}}$ over time with Eq. (4). The x-axis represents the days from the first day of the observed data. We show that the estimated DoD tended to increase until the hydraulic pump was replaced. The broken hydraulic pump was caused by wear of the piston surface. Then, after the pump was replaced, the DoD recovered.

These results demonstrate that the proposed method succeeded in identifying the trend of the deterioration of the hydraulic pump.

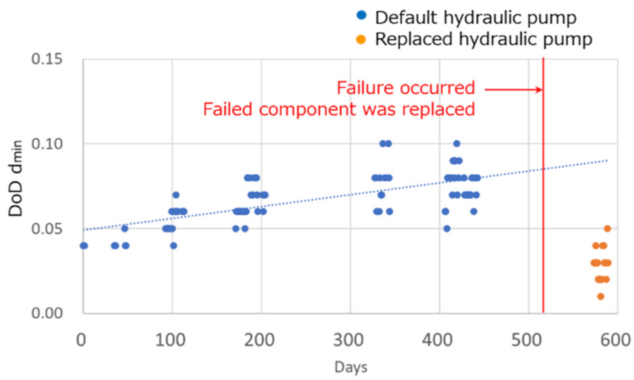

Fig. 10. Relationship between estimated DoD $\boldsymbol{d_{min}}$ and days from first day of observed data.

4. Discussion

Our method dealt with a physical model and hyperplane created from simulated data in state space.

When the DoD is identified, the physical model allows us to reason about the machine system to address interpretability. In our case study, the estimated DoD and the physical model told us how the piston condition deteriorated. This is because the pump volumetric efficiency described as DoD is related to the degree of piston surface wear.

Then, in the preparation phase, we constructed 20 hyperplanes in the state space with the historical data only under normal machine behavior and the simulated data. Using the hyperplanes, we verified that our method identified the trend of the deterioration of the hydraulic pump. As a result, our method addressed the issue with data dependency.

Furthermore, our method succeeded in addressing two issues described in Section 1. First, it filled the gap between historical and simulated data to minimize the difference between the hyperplane of historical data and that of simulated data. As a result, we succeeded in building a physical model that achieved a high correlation coefficient between simulated and historical data.

One of the key criteria on the level of validity of the physical model is the correlation coefficient of simulated and observed data. In this case study, we built the physical model to achieve the correlation coefficient over 0.9.

Second, the state space clarified the relationship among input (rotational speed and desired pump pressure), observable state variables (drain pressure), and DoD. Time series data of multiple operation modes were mapped onto the hyperplane in the state space. As a result, we successfully estimated the DoD with the state space regardless of the machine operation mode.

Our method can be applied to various machine systems under the following condition. First, attributes of deterioration are defined in the physical model. Then, input and output data of the physical model are observed from the physical world. Finally, the machine system has multiple operation modes.

However, our method has potential limitations. For example, it dealt with a single failure mode and deterioration that was assumed to progress in accordance with time. Multiple failure modes need to be considered in the future. Moreover, the accuracy of our method depends on the physical model preciseness. In our case study, we built the simple physical model of hydraulic pump based on the design information and discussion with domain engineers. Future study should clarify a level of model preciseness and design information to apply our method.

5. Conclusions

For condition monitoring systems, we proposed a physical model-based method for estimating deterioration with a CPS. Then, in a case study, we demonstrated the feasibility of the proposed method for estimating the deterioration of an actual machine system, a mining machine, with actual data.

The advantages of the proposed method include identifying the degree of deterioration in machinery that has multiple operation modes, as well as addressing interpretability and data dependency.

In future work, we will deal with multiple failure modes for condition-based maintenance.

References:

[1] Y. Umeda, S. Takata, F. Kimura, T. Tomiyama, J. W. Sutherland, S. Kara, C. Herrmann, and J. R. Duflou, "Toward Integrated Product and Process Life Cycle Planning – An Environmental Perspective," CIRP Annals-Manufacturing Technology, Vol.61, No.2, pp. 681-702, 2012.

[2] E. Kunii, T. Matsuura, S. Fukushige, and Y. Umeda, "Proposal of Consistency Management Method Between Product and its Life Cycle for Supporting Life Cycle Design," Int. J. Automation Technol., Vol.6, No.3, pp. 272-278, 2012.

[3] A. Bousdekis, B. Magoutas, D. Apostolou, and G. Mentzas, "Review, Analysis and Synthesis of Prognostic-based Decision Support Methods for Condition Based Maintenance," J. of Intelligent Manufacturing, Vol.29, pp. 1303-1316, 2018.

[4] E. Kharlamov, T. Mailis, G. Mehdi, C. Neuenstadt, Ö. Özçep, M. Roshchin, N. Solomakhina, A. Soylu, C. Svingos, S. Brandt, M. Giese, Y. Ioannidis, S. Lamparter, R. Möller, Y. Kotidis, and A. Waaler, "Semantic Access to Streaming and Static Data at Siemens," J. of Web Semantics, Vol.44, pp. 54-74, 2017.

[5] R. Roy, R. Stark, K. Tracht, S. Takata, and M. Mori, "Continuous Maintenance and the Future – Foundations and Technological Challenges," CIRP Annals-Manufacturing Technology, Vol.65, No.2, pp. 667-688, 2016.

[6] L. Tang, T. Li, L. Shwartz, F. Pinel, and G. Grabarnik, "An Integrated Framework for Optimizing Automatic Monitoring Systems in Large IT Infrastructures," KDD'13, pp. 1249-1257, 2013.

[7] T. Hiruta, T. Uchida, S. Yuda, and Y. Umeda, "A Design Method of Data Analytics Process for Condition Based Maintenance," CIRP Annals-Manufacturing Technology, Vol.68, No.1, pp. 145-148, 2019.

[8] D. Djurdjanovic, J. Lee, and J. Ni, "Watchdog Agent – An Infotronics-based Prognostics Approach for Product Performance Degradation Assessment and Prediction," Advanced Engineering Informatics, Vol.17, Issues 3-4, pp. 109-125, 2003.

[9] S. Wegerich, "Similarity-based Modeling of Vibration Features for Fault Detection and Identification," Sensor Review, Vol.25, No.2, pp. 114-122, 2005.

[10] F. Xue and W. Yan, "Parametric Model-based Anomaly Detection for Locomotive Subsystems," Proc. of Int. Joint Conf. on Neural Networks, 2007.

[11] R. Sipos, D. Fradkin, F. Moerchen, and Z. Wang, "Log-based Predictive Maintenance," KDD'14, pp. 1867-1876, 2014.

[12] C. Sobie, C. Freitas, and M. Nicolai, "Simulation-driven Machine Learning: Bearing Fault Classification," Mechanical Systems and Signal Processing, Vol.99, pp. 403-419, 2018.

[13] M. Yu, D. Wang, M. Luo, and L. Huang, "Prognosis of Hybrid Systems with Multiple Incipient Faults: Augmented Global Analytical Redundancy Relations Approach," IEEE Trans. on Systems Man and Cybernetics, Part A: Systems and Humans, Vol.41, No.3, pp. 540-551, 2011.

[14] A. Saxena, K. Goebel, D. Simon, and N. Eklund, "Damage Propagation Modeling for Aircraft Engine Run-to-Failure Simulation," Int. Conf. on Prognostics and Health Management, 2008.

[15] J. Lee, B. Bagheri, and H. Kao, "A Cyber-physical Systems Architecture for Industry 4.0-based Manufacturing Systems," Manufacturing Letters, Vol.3, pp. 18-23, 2015.

[16] S. Vetra-Carvalho, P. J. v. Leeuwen, L. Nerger, A. Barth, M. U. Altaf, P. Brasseur, P. Kirchgessner, and J. Beckers, "State-of-the-art Stochastic Data Assimilation Methods for High-dimensional Non-Gaussian Problems," Tellus A: Dynamic Meteorology and Oceanography, Vol.70, Issue 1, pp. 1-43, 2018.

[17] T. Tsuyuki and T. Miyoshi, "Recent Progress of Data Assimilation Methods in Meteorology," J. of the Meteorological Society of Japan, Vol.85B, pp. 331-361, 2007.

[18] H. Arabian-Hoseynabadi, H. Oraee, and P. J. Tavner, "Failure Modes and Effects Analysis (FMEA) for Wind Turbines," Electrical Power and Energy Systems, Vol.32, Issue 7, pp. 817-824, 2010.

[19] T. Kato, "Characteristics and Applications of Controlled Volume Pumps," Turbomachinery, Vol.17, Issue 9, pp. 576-582, 1989 (in Japanese).

[20] M. E. Klenk, J. de Kleer, D. Bobrow, and B. Janssen, "Qualitative Reasoning with Modelica Models," AAAI'14 Proc. of the Twenty-Eighth AAAI Conf. on Artificial Intelligence, pp. 1084-1090, 2014.

[21] https://www.modelica.org/ [Accessed June 1, 2020]

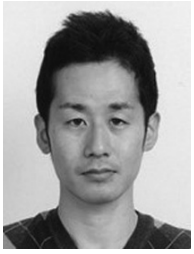

Name:
Tomoaki Hiruta

Affiliation:
Senior Researcher, Research & Development Group, Hitachi Ltd.

Address:
7-1-1 Omika-cho, Hitachi, Ibaraki 319-1292, Japan

Brief Biographical History:
2005- Hitachi Research Lab., Hitachi, Ltd.
2015- Researcher, Big Data Research Lab., Hitachi America, Ltd.
2017- Senior Researcher, Center for Technology Innovation – Controls, Research and Development Group, Hitachi, Ltd.

Main Works:
• "A Design Method of Data Analytics Process for Condition Based Maintenance," CIRP Annals – Manufacturing Technology, Vol.68, Issue 1, pp. 145-148, 2019.

Membership in Academic Societies:
• Japan Society of Mechanical Engineers (JSME)

Name:
Yasushi Umeda

Affiliation:
Professor, Research into Artifacts, Center for Engineering, School of Engineering, The University of Tokyo

Address:
7-3-1 Hongo, Bunkyo, Tokyo 113-8656, Japan

Brief Biographical History:
1992 Received Dr. of Eng. from The University of Tokyo
1992- Research Associate / Lecturer, The University of Tokyo
1999- Associate Professor, Tokyo Metropolitan University
2005- Professor, Osaka University
2014- Professor, The University of Tokyo

Main Works:
• "Modeling competitive market of remanufactured products," CIRP Annals – Manufacturing Technology, Vol.66, Issue 1, 2017.
• "An analysis of remanufacturing practices in Japan," J. of Remanufacturing, Vol.1, No.2, 2011.
• "Analysis of Reusability using 'Marginal Reuse Rate'," CIRP Annals Manufacturing Technology, Vol.55, Issue 1, pp. 41-44, 2006.
• "Supporting Conceptual Design Based on the Function Modeler," AIEDAM, Vol.10, No.4, pp. 275-288, 1996.

Membership in Academic Societies:
• American Society of Mechanical Engineers (ASME)
• International Academy for Production Engineering (CIRP), Fellow
• Design Society (DS)
• Japan Society of Mechanical Engineers (JSME), Fellow
• Japan Society for Precision Engineering (JSPE)